Proceedings of the ASME 2010 3rd Joint US-European Fluids Engineering Summer Meeting and 8th International Conference on Nanochannels, Microchannels, and Minichannels
FEDSM-ICNMM2010
August 1-5, 2010, Montreal, Canada

FEDSM-ICNMM2010-30778

ANALYTICAL TREATMENT OF HEAT TRANSFER IN ELECTROKINETIC FLOWS

Jafar Jamaati
Ferdowsi University of Mashhad
Mechanical Engineering Department
Mashhad, Iran

Hamid Niazmand
Ferdowsi University of Mashhad
Mechanical Engineering Department
Mashhad, Iran

Metin Renksizbulut
University of Waterloo
Mechanical & Mechatronics Engineering Department
Waterloo, Ontario, Canada

ABSTRACT

This paper investigates the effects of velocity slip in the presence of an electric double-layer on fluid flow and heat transfer in a parallel plate hydrophobic microchannel. The electric potential filed is determined through the Poisson-Boltzmann equation together with the Debye-Hückel (D-H) approximation, while the velocity field is obtained by solving the Navier-Stokes equations under fully developed conditions. In most previous studies, zeta-potential has been considered as an independent variable for the analysis of induced voltage. However, experimental findings show that in electrokinetic slip flows with constant wall potential, the zeta potential is related to the slip coefficient and the D-H parameter. Therefore, in the present study, the wall potential is considered as an independent variable and the zeta potential is determined from an available experimental correlation. The effects of velocity slip, the D-H parameter, the wall potential and the Brinkman number on the induced voltage and the velocity and temperature fields are examined in detail. Results indicate that the slip effects on the zeta potential dramatically affect the flow and temperature fields.

NOMENCLATURE

B	ratio of ionic pressure to dynamic pressure, $k_b T_{ref} n_0/\rho U_{ref}^2$
Br	Brinkmann number $Br = \mu U_{ref}^2/k\,\Delta T_{ref}$
D	species diffusion coefficient, $[m^2/s]$
e	elementary charge, 1.602×10^{-19}, [C]
E_x	induced voltage, $E_x^*/(\psi_{ref}/H)$
H	microchannel height, [m]
K	dimensionless Debye-Hückel parameter, κH
k	thermal conductivity, [W/mK]
k_b	Boltzmann constant, 1.381×10^{-23}, [J/K]
n_0	bulk ionic concentration, $[ions/m^3]$
P	pressure, $P^*/\rho U_{ref}^2$
Pr	Prandtl number, ν/α
q_s	surface charge density, $q_S^*/H\rho_{e,ref}$
Re	Reynolds number, $\rho U_{ref} H/\mu$
Sc	Schmidt number, $\mu/\rho D$
T	absolute temperature, T^*/T_{ref}
T_{ref}	reference temperature, 298 K
u	axial velocity, u^*/U_{ref}
U_{ref}	reference velocity, $-(dP^*/dx^*)H^2/8\mu$, [m/s]
x, y	Cartesian coordinates, x^*/H, y^*/H
z	valance number of ions for a symmetric electrolyte, $z = \lvert z^+\rvert = \lvert z^-\rvert = 1$

Greek symbols

α	thermal diffusivity, $[m/s^2]$
β	slip coefficient, β^*/H
ε_0	permittivity of vacuum, 8.854×10^{-12} [C/Vm]
ε_r	relative dielectric constant of the electrolyte, $\varepsilon_r = 78.5$
ϕ	induced electric potential, ϕ^*/ψ_{ref}
κ	Debye-Hückel parameter, $ze(2n_0/\varepsilon_r\varepsilon_0 k_b T_{ref})^{1/2}$, [1/m]
μ	dynamic viscosity, $[Ns/m^2]$
ρ	fluid density, $[kg/m^3]$
ρ_e	net electric charge density, $\rho_e^*/\rho_{e,ref}$
$\rho_{e,ref}$	reference charge density, zen_0, $[C/m^3]$
σ_e	local electrical conductivity, σ_e^*/σ_{ref}
σ_{av}	average electrical conductivity at cross section, $\sigma_{av}^*/\sigma_{ref}$

σ_{ref} reference conductivity, $Dz^2e^2n_0/k_bT_{ref}$, $[1/\Omega m]$
ψ electric potential, ψ^*/ψ_{ref}
Ψ total electric potential, Ψ^*/ψ_{ref}
ψ_{ref} reference electrical potential, k_bT_{ref}/ze, [V]
ζ zeta-potential, ζ^*/ψ_{ref}
θ dimenssionless temperature $(T - T_w)/\Delta T_{ref}$

Superscripts and Subscripts

$*$ dimensional quantity
$'$ derivative d/dy
c mid-plane value
w at the wall

INTRODUCTION

Microfluidic systems have become increasingly attractive in a variety of engineering fields due to recent advances in microfabrication technologies. Precise control of such systems often requires a complete understanding of the interaction between fluid dynamics and the electrical properties of the microchannel; usually referred to as electrokinetics. In every electrokinetic application, finding the accurate distribution of the prevailing electric potential is of fundamental importance, which is governed by the non-linear Poisson-Boltzmann (P-B) equation. The linear form, following the Debye-Hückel (D-H) approximation, is valid when the electrical potential is small compared to the thermal energy of the ions.

Different methods have been developed for the solution of the P-B equation. Exact solution of the P-B equation between two dissimilar planar charged surfaces is presented by Behrens and Borkovec [1] in terms of Jacobian elliptic functions. A similar approach has been employed by other researchers [2,3] for the evaluation of streaming current and electrokinetic energy conversion. There have been several attempts to extend the analytical solution of the P-B equation for a single flat plate [4] to a planar microchannel with overlapping electric double-layers (EDL) [5-7]

Experimental studies, which are reviewed by Neto et al. [8], have shown the existence of significant liquid slip at the walls when low-energy (hydrophobic) surfaces are involved even at low Reynolds numbers ($Re < 10$) [9,10]. Bouzigues et al. [11] presented experimental evidence for slip-induced amplification effects on the wall zeta-potential. It was demonstrated that slip leads to amplification of the zeta potential by a factor of $(1 + K\beta)$, which indicates considerable increase in the zeta-potential especially for larger K (see Nomenclature). This fact is also confirmed by the theoretical model presented by Chakraborty [12] based on the free energy for binary mixtures. Slip effects have been studied in microchannel flows, and the results indicate an increase in the mass flow rate and considerable reduction in the applied voltage for electro-osmotic flows [13].

Electrokinetic flows have been mostly studied in the context of electro-osmotic flows, which involve applied electric fields but no externally applied pressures gradients. In electro-osmotic flows, the induced electric potential due to fluid motion is negligible in comparison to the applied electric potential. On the other hand, in purely pressure-driven flows, a significant electric potential can be generated due to the motion of charged fluid particles, which is called the streaming potential [14]. This potential serves as the basis for possible micro-scale power generators or batteries. Very limited information is available in the literature regarding the combined effects of zeta-potential and slip at the walls on the streaming potential in purely pressure-driven flows [15].

The thermal aspects of electrokinetic liquid flows in microchannel are studied mostly in the context of Joule-heating [5,16] in which an applied electric field along the channel results in a volumetric heating in the fluid. Maynes and Webb [16] studied the temperature fields in electro-osmotic flow and analytically investigated the Nusselt number in both flat microchannels and circular micro-tubes. Jain and Jenson [17] analytically studied the fluid flow and heat transfer in a microchannel with a thick EDL in no-slip flows and investigated the effects of the EDL and the zeta-potential on the friction factor and Nusselt number. Elazhary and Soliman [7] performed a similar study for a microchannel with high zeta-potential and considered viscous dissipation in the energy equation; however, the effects of liquid slip on heat transfer were not considered.

In the present study, the effects of slip at the walls on the velocity and temperature fields, and on the induced voltage are studied for fully developed flows in flat hydrophobic microchannels. Similar to recent studies [11,12], the effects of slip on the zeta potential are included in the present analysis.

MATHEMATICAL FORMULATION

Consider the pressure-driven slip-flow of an incompressible Newtonian aqueous 1:1 electrolyte of uniform dielectric constant between parallel plates (flat microchannel) with uniform wall potential Ψ_w and slip coefficient β at both walls as shown in Fig.1.

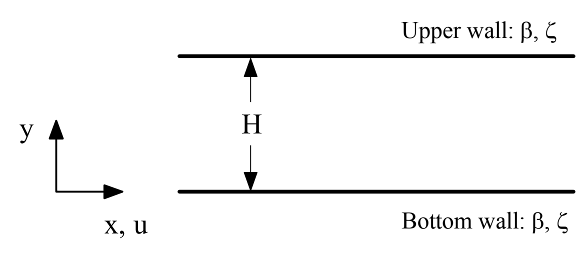

Fig. 1: Microchannel geometry and the coordinate system.

The flow is considered to be steady, laminar, and fully developed. Heat transfer takes place due to a uniform heat flux q" imposed at both walls. Solutions of the electric potential field are obtained based on the well-known Debye–Hückel approximation, since the velocity and temperature fields can then be expressed in relatively simple closed-form solutions allowing for a better analysis of the physical aspects of the problem. The Navier-Stokes equations with an electrical body force are solved for the velocity field, while the energy equation with viscous dissipation terms is solved for the temperature distribution.

THE ELECTRIC POTENTIAL FIELD

According to the theory of electrostatics, the relationship between the total electric potential Ψ and the local net charge density per unit volume ρ_e at any point in an electrolyte solution is described by the Poisson equation:

$$\nabla^2\Psi = -K^2\rho_e/2 \quad (1)$$

In general, the total electrical potential can be expressed as:

$$\Psi = \psi + \phi \quad (2)$$

where ψ is due to the EDL at an equilibrium state (i.e., no liquid motion and no externally applied electric field) and ϕ is the flow-induced electric potential. It can be shown that for fully-developed conditions, the electrical potential variation in the flow direction can be at most linear. Therefore, $\phi = -E_x x$ where $E_x = -\partial\Psi/\partial x$ is the strength of the electric field. Based on the Boltzmann distribution of charges in the EDL, and in the absence of non-electrical work, the net charge density is given by:

$$\rho_e = -2\sinh(\psi) \quad (3)$$

Substitution of Eq. (3) into the Poisson equation leads to the well-known Poisson-Boltzmann equation:

$$\frac{d^2\psi}{dy^2} = K^2\sinh(\psi) \quad (4)$$

where $K = \kappa H = zeH(2n_0/\varepsilon_0\varepsilon_r k_b T_{ref})^{1/2}$ is the dimensionless Debye-Hückel parameter which is independent of the wall properties and is determined by the electrolyte and the geometric scale of the problem. The electric potential distribution is obtained by solving Eq. (4) subject to appropriate boundary conditions. Subsequently, the charge density distribution ρ_e is determined from Eq. (3). For the case of low zeta potential with $\sinh(\psi) \approx \psi$, the solution of Eq. (4), known as the Debye-Hückel solution, is obtained as:

$$\psi(y) = \zeta\frac{\cosh(Ky - K/2)}{\cosh(K/2)} \quad (5)$$

THE FLOW FIELD

The solution to the linear P-B equation discussed above has been employed for the analytical treatment of heat transfer in pressure-driven flows with slip. For the case of a steady fully-developed liquid flow through a planar microchannel, the equation of motion reduces to:

$$\mu\frac{d^2u^*}{dy^{*2}} - \frac{dP^*}{dx^*} + B\rho_e E_x^* = 0 \quad (6)$$

Using the classical Poiseuille-flow maximum velocity $U_{max} = (-dP^*/dx^*)(H^2/8\mu)$ as reference, and introducing the charge density from Eq. (3), the momentum equation takes the following form:

$$\frac{d^2u}{dy^2} = \frac{2BReE_x}{K^2}\left(\frac{d^2\psi}{dy^2}\right) - 8 \quad (7)$$

where $B = k_b T_{ref} n_0/\rho U_{ref}^2$ is the ratio of the osmotic pressure to the dynamic pressure. Noting that E_x is constant under fully-developed conditions and solving Eq. (7) assuming slip at the walls $(u = \beta du/dy)$ and symmetry condition at mid-plane $(du/dy = 0)$, the following velocity profile is obtained:

$$u = 4\left\{y - y^2 - G\left(1 - \frac{\psi}{\zeta}\right) + \beta\left(1 - \frac{GK^2q_S}{2\zeta}\right)\right\} \quad (8)$$

where $G = BReE_x\zeta/2K^2$ and $q_S = \int_0^{1/2}\rho_e(y)dy = -2\psi'(0)/K^2$ is the charge density at the wall. The first term in Eq. (8) is due to the applied pressure gradient. The second term represents the contribution of the EDL to the velocity profile and the third term reflects the slip effect. However, the coefficient G is indirectly related to the slip effect through the resulting induced voltage. From Eq. (8), the slip velocity at the wall is found to be:

$$u_S = 4\beta\left(1 - \frac{BReE_x q_S}{4}\right) \quad (9)$$

THE TEMPERATURE FIELD

The energy equation for steady, laminar, and hydrodynamically and thermally fully-developed conditions is given by:

$$u^*\frac{\partial T^*}{\partial x^*} = \alpha\left(\frac{\partial^2 T^*}{\partial x^{*2}} + \frac{Pr}{C_p}\left(\frac{du^*}{dx^*}\right)^2\right) \quad (10)$$

For the case of a uniform applied heat flux, performing an overall energy balance leads to an expression for the axial temperature gradient $\partial T^*/\partial x^*$ in terms of the wall heat flux and cross-sectional viscous dissipation as given below:

$$\frac{\partial T^*}{\partial x^*} = \frac{dT_m^*}{dx^*} = \frac{2q''}{\rho U_m^* C_p H}\left[1 + \frac{\mu}{2q''}\int_0^H\left(\frac{du^*}{dy^*}\right)^2 dy^*\right] \quad (11)$$

Substitution of Eq. (11) into the energy equation (10) and using dimensionless parameters, the energy equation becomes:

$$\frac{d^2\theta}{dy^2} + \frac{u}{U_m}[1 + BrJ\,] = Br\left(\frac{du}{dy}\right)^2 \tag{12}$$

where Br is a modified Brinkman number and $J = \int_0^1 (du/dy)^2 dy$ is due to viscous dissipation. The boundary conditions for Eq. (12) are: $\theta = 0$ at $y = 0$ and $d\theta/dy = 0$ at $y = 1/2$. Using the velocity distribution given by Eq. (8) and the potential distribution given by Eq. (5), the solution of energy equation can be obtained as a function of y . However, this function can be expressed in a more simple form in terms of $z = 1 - 2y$ as follows:

$$\theta(z) = C_0 + \frac{(1+BrJ)}{2U_m}\left\{C_0\beta\zeta\frac{z^2}{2} - \frac{z^4}{12} + \frac{16G}{K^2}\frac{\Psi}{\zeta}\right\} - 4Br\left\{\frac{z^4}{12} - \frac{16G}{K^2\zeta}\left(\frac{d\Psi}{dz} - 2\Psi\right) + \frac{K^2G^2}{2\left(\cosh\left(\frac{K}{2}\right)\right)^2}\left(\frac{\cosh(Kz)}{K^2} - \frac{z^2}{2}\right)\right\} \tag{13}$$

where C_0 is a constant obtained from the boundary condition at the wall.

RESULTS

To obtain the temperature field in electrokinetic flows, the potential field is calculated first using Eq. (5). The solution is then introduced into the momentum equation to account for the streaming potential effects. Different solutions of potential field that is governed by P-B equation have been developed so far, which are reviewed in [15]. Here the P-B solution based on the commonly used D-H approximation is adopted, since the velocity and temperature fields can then be expressed in closed-form analytical expressions. For all cases considered here, Re=1 and Sc=500 are used in the analysis.

The key parameter in electrokinetic flows with streaming potential is the induced voltage which has been found to be a function of different parameters such as the zeta-potential, the D-H parameter, the slip coefficient, the averaged electrical conductivity and various flow parameters. In most previous studies, the zeta-potential has been considered as an independent variable for the analysis of induced voltage. However, experimental findings show that in electrokinetic slip flows with constant wall potential (Ψ_w), the zeta-potential is related to the slip coefficient, D-H parameter, and wall potential according to $\zeta = \Psi_w(1 + K\beta)$. This relation is proposed by [11,12] and has been adopted in the present study. The fact that zeta potential is influenced by the slip coefficient and D-H parameter for a constant wall potential opens up a new window for re-examination of the induced voltage and its relevant parameters as will be discussed later.

For this matter, in Fig. 2 the variations of induced voltage with slip coefficient for various values of wall potentials based on the D-H approximation are plotted. According to the D-H approximation, the electrical conductivity (σ_e) is considered as a constant in the whole potential filed and consequently $\sigma_{av} = 2$ is employed. For this value of σ_{av} , it can be seen from Fig. 2 that the induced voltage increases as the slip coefficient increases up to a maximum value, but then decreases at higher slip coefficients. Clearly, the slip coefficient corresponding to the maximum induce voltage depends on the value of the wall potential. Furthermore, this figure shows that the maximum induced voltage is higher at lower wall potentials and higher slip coefficients. Although $\sigma_{av} = 2$ correctly predicts the trends of induced voltage variations as the slip coefficient and wall potential vary, it greatly over estimates the induce voltage quantitatively, as indicated by Mirbozorgi et al. [14] as well. One remedy is a more accurate evaluation of the averaged electrical conductivity by performing a numerical integration of $\sigma_{av} = \int 2\cosh(\psi)\,dy$. The result can then be used in the calculation of induced voltage shown in Fig. 3. A comparison of Figs. 2 and 3 clearly shows that the assumption of constant electrical conductivity ($\sigma_{av} = 2.0$) results in a considerable over-prediction of the induced voltage. For example, at $\beta = 0.05$ and $\Psi_w = -75\text{mV}$, from Fig. 2, the absolute value of induced voltage is about $|E_X| = 50$, which is 150% more than $|E_X| = 20$ obtained from Fig. 3.

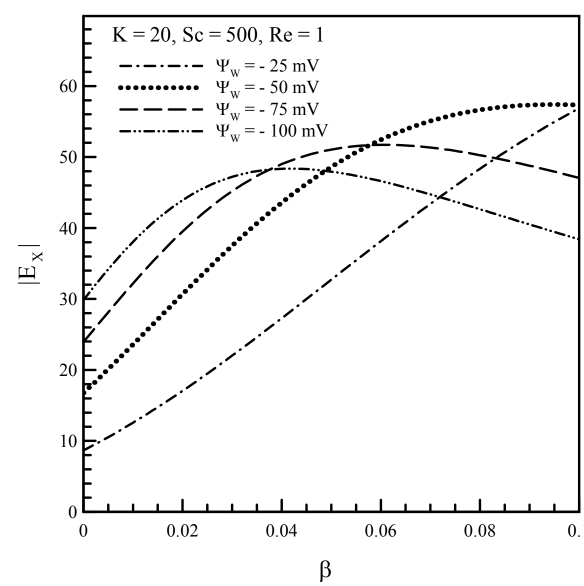

Fig. 2: Induced voltage as a function of slip coefficient for various wall potentials with $\sigma_{av} = 2$.

A contour map of induced voltage reveals its characteristics more clearly as shown in Fig. 4. It is notable that in regions of low wall potential ($|\Psi_W| < 50\text{mV}$), the induced voltage increases continuously as the slip coefficient increases. On the other hand, for large values of wall potential ($|\Psi_W| > 100mV$) the induced voltage decreases almost continuously as slip coefficient increases. The values of dimensionless induced voltage are at most 20 in the region of high wall potentials. More interesting region is the region of the intermediate wall potential ($50\mathrm{mV} < |\Psi_W| < 100mV$). In this region, at a given wall potential, the induced voltage rapidly increases as slip coefficient increases up to a maximum value and then decreases gradually at higher slip coefficients. These results are considerably different from previous predictions of induced voltage in which the zeta-potential dependence on the slip coefficient and the D-H parameter is ignored [2]. More importantly, this figure shows that large wall potentials are not required to obtain large values of induced voltage. Clearly, moderate values of wall potentials ($|\Psi_W| \approx 30\mathrm{mV}$) at relatively large slip coefficients ($\beta \approx 0.1$) generate large induced voltages. Consistent with previous studies for the no-slip condition ($\beta = 0$), maximum induced voltage occurs at large wall potentials of about $|\Psi_W| \approx 80\mathrm{mV}$.

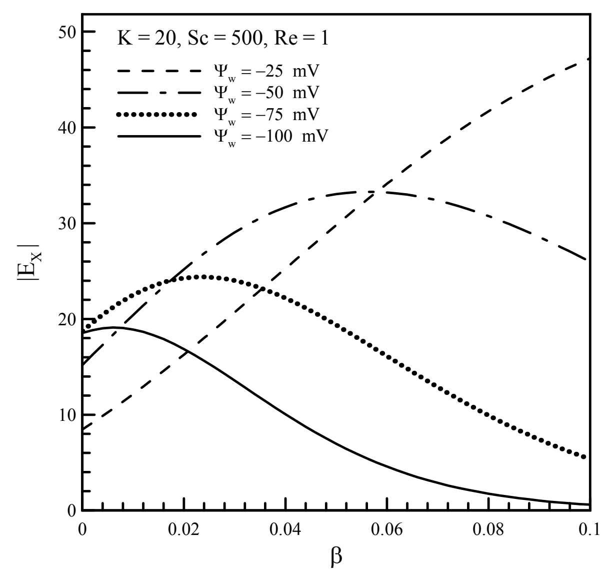

Fig. 3: Induced voltage as a function of slip coefficient for various wall potentials with $\sigma_{av} = \int 2\cosh(\psi)\, dy$

Prior to discussing the thermal field, the velocity field is briefly examined as a function of the wall potential. In Fig. 5, the velocity profiles across the channel for different wall potentials are plotted for $K = 20$ and $\beta = 0.1$. This figure shows that velocity-slip decreases as the magnitude of the wall potential increases, while the trend is reversed at higher wall potentials.

This can be explained by the fact that induced voltage generates a flow that always opposes the pressure driven flow. According to Eq. (9) it is clear that increasing induced voltage results in reducing the velocity-slip. Moreover, from Fig. 4, it can be seen that at a given slip coefficient, the induced voltage increases as the wall potential increases up to a certain value and then decreases at higher wall potentials. Therefore, similar behavior is expected for the velocity-slip.

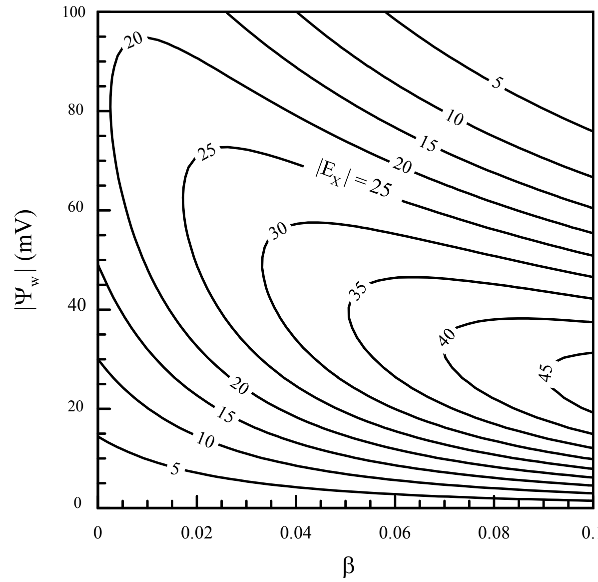

Fig. 4: Contours of induced voltage as a function of slip coefficient and wall potential for K=20.

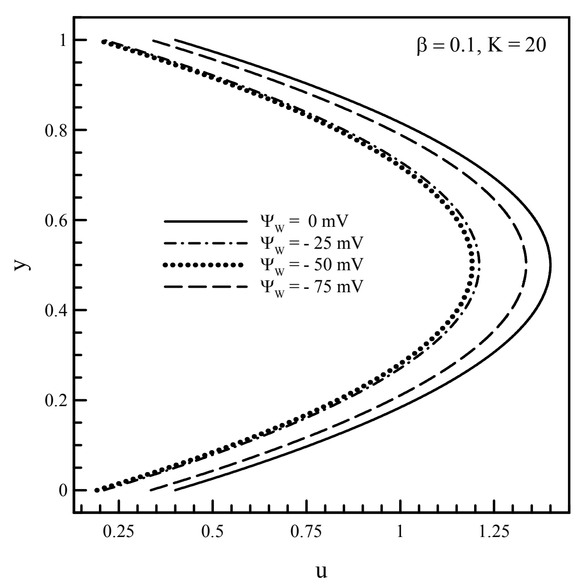

Fig. 5: The effect of wall potential (Ψ_w) in slip flows on the velocity distribution

The effects of slip and wall potential on the temperature field are considered with the help of the contour maps of the mid-plane temperature as shown in Fig 6. Similar patterns to the contour maps of induced voltage are observed in this figure indicating that different scenarios may be encountered in electro-kinetic slip flows. It is important to note that the contour maps would be totally different if constant electrical conductivity ($\sigma_e = 2.0$) were considered. According to this figure, the minimum mid-plane temperature occurs in the region of larger values of the slip coefficient and lower wall potentials; indicating that the presence of slip and wall potential affect viscous dissipation in opposing directions, that is, the former strengthens while the later weakens it.

Since the effects of slip on the temperature field have not been considered in previous studies, temperature profiles for different values of the slip coefficient are presented in Fig. 7. In this figure, the temperature profiles are related to the condition where a relatively large wall potential ($\Psi_w = -75$ mV) with a somewhat thick EDL (K=20) exist in a channel with heat transfer to the fluid ($\mathrm{Br} = -1$). It should be noted that the trend of the temperature variations is reversed as the slip coefficient increases, and that the temperature of the channel core increases due to viscous dissipation.

The effects of some variables, such as the wall potential and the D-H parameter, on the temperature field are relatively limited. However, the temperature field is strongly influenced by the Brinkman number. Note that a positive Brinkman number corresponds to a fluid cooling case, while a negative Br corresponds to a fluid heating condition. For a given slip coefficient and wall potential, the temperature profiles are plotted for different values of Brinkman number in Fig. 8. At higher Brinkman numbers, the fluid temperatures are lower than the wall temperature everywhere as seen in this figure.

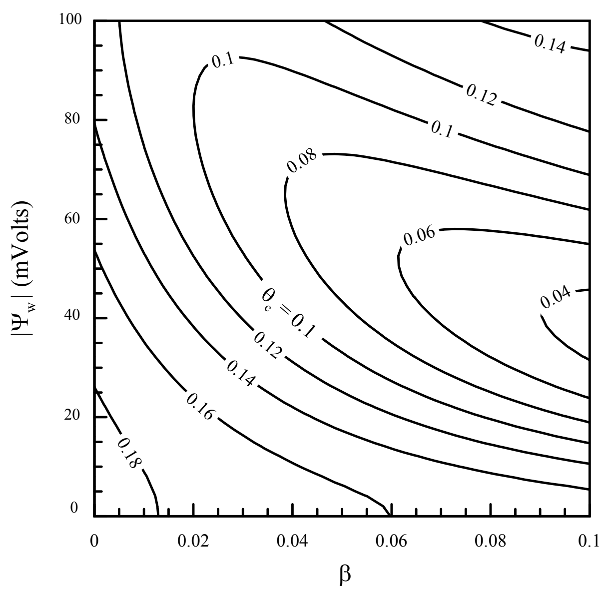

Fig. 6: Contours of dimensionless mid-plane temperature as a function of slip coefficient (β) and wall potential (Ψ_w) for K=20 and $\mathrm{Br} = -1$

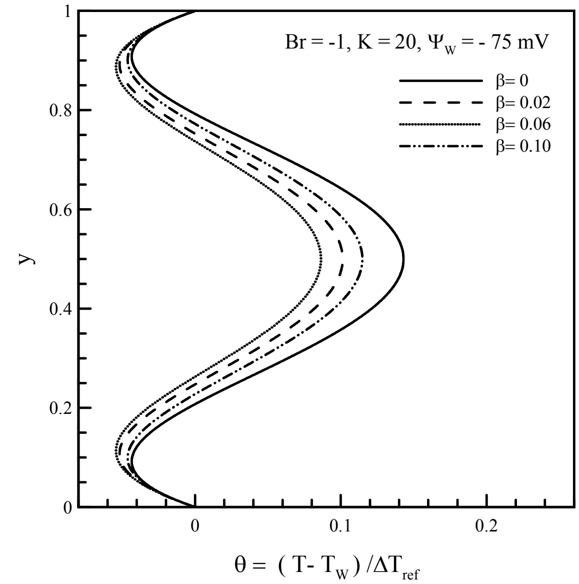

Fig. 7: Dimensionless temperature distribution across the channel for various slip coefficients

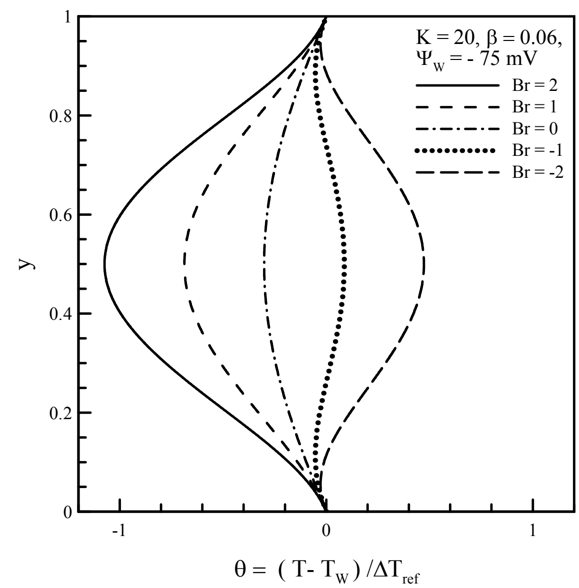

Fig. 8: Dimensionless temperature distribution across the channel for various values of the Brinkman number.

CONCLUSION

In the present work, the effect of slip at the walls on the induced voltage and on the velocity and temperature fields are studied in fully developed electrokinetic flows in flat hydrophobic microchannels.

The results indicate that the EDL (characterized by the Debye-Hückel parameter and the zeta-potential) influences the velocity filed through the induced voltage and this effect intensifies in the presence of slip. It is found that for slip flows, highest induced voltages occur at relatively low wall potentials (~25mV), which is totally different than no-slip flows in which higher induced voltages occur at quite large wall potentials (~80mV).

It is found that the common assumption of $\sigma_{av} = 2.0$ in the Debye-Hückel approximation can lead to serious errors in the calculation of the induced voltage and the velocity and temperature fields, which can be prevented if electrical conductivity is calculated through a simple numerical integration in which its variation with wall potential is considered.

Investigation of the temperature field showed that slip, wall potential and the Debye-Hückel parameter affect the temperature distribution significantly. The dimensionless Brinkman number is used to study the heating/cooling conditions at the walls. A parametric study of the temperature field with viscous dissipation indicates that at higher Brinkman numbers, for which viscous dissipation is dominant over the wall heating/cooling effect, significant temperature variations can occur across the channel which may require the use of temperature dependent thermo-physical properties.

ACKNOWLEDGMENT

The financial support of the Ferdowsi University of Mashhad and the Natural Sciences and Engineering Research Council of Canada (NSERC) are gratefully acknowledged.

REFERENCES

[1] Behrens, S.H., and Borkovec, M., 1999, “Exact Poisson-Boltzmann solution for the interaction of dissimilar charge-regulating surfaces,” Physical Review E, 60(6), pp. 7040-7048.

[2] Davidson, C., and Xuan, X., 2008, “Electrokinetic energy conversion in slip nanochannels,” Journal of Power Sources, 179 (2008) 297-300.

[3] Ren, Y., and Stein, D., “Slip-enhanced electrokinetic energy conversion in nanofluidic channels,” Nanotechnology, 19, pp. 195707(6).

[4] Hunter, R.J., 1981, Zeta-potential in Colloid Science: Principles and Applications, Academic Press, London.

[5] Dutta, P., Horiuchi, K., and Yin, H.M., 2006, “Thermal characteristics of mixed electroosmotic and pressure-driven microflows,” Computers and Mathematics with Applications, 52(5), pp. 651-670.

[6] Dutta, P., and Beskok, A., 2001, “Analytical solution of combined electroosmotic/pressure driven flows in two-dimensional straight channels: Finite Debye layer effects,” Analytical Chemistry, 73(9), pp. 1979-1986.

[7] Elazhary, A., and Soliman, H.M., 2009, “Analytical solutions of fluid flow and heat transfer in parallel-plate micro-channels at high zeta-potentials,” International Journal of Heat and Mass Transfer, 52, pp. 4449–4458.

[8] Neto, C., Evans, D.R., Bonaccurso, E., Butt, H.J., and Craig, V.S., 2005, “Boundary slip in Newtonian liquids: a review of experimental studies,” Report on Progress in Physics, 15, pp. 2859-2897.

[9] Tretheway, D.C., and Meinhart, C.D., 2004, “A generating mechanism for apparent fluid slip in hydrophobic microchannels,” Physics of Fluids, 16(5), pp. 1509-1515.

[11] Bouzigues, C.I., Tabeling, P., and Bocquet, L., 2008, “Nanofluidics in the debye layer at hydrophilic and hydrophobic surfaces,” Physical Review Letters, 101(11), pp. 114503(4).

[10] Holt, J.K., Park, H.G., Wang, Y., Stadermann, M., Artyukhin, A.B., Grigoropoulos, C.P., Noy, A., and Bakajin, O., 2006, “Fast mass transport through sub-2-nanometer carbon nanotubes,” Science, 312(5776), pp. 1034-1037.

[12] Chakraborty, S., 2008, “Generalization of interfacial electrohydrodynamics in the presence of hydrophobic interactions in narrow fluidic confinements,” Physical Review Letters, 100(9), pp. 097801(4).

[13] Yang, J., and Kwok, D.Y., 2003, “Effect of liquid slip in electrokinetic parallel-plate microchannel flow,” Journal of Colloid and Interface Science, 260(1), pp. 225-233.

[14] Mirbozorgi, S.A., Niazmand, H., and Renksizbulut, M., 2007, “Streaming electric potential in pressure-driven flows through reservoir-connected microchannel,” Journal of Fluids Engineering, Transactions of the ASME, 129(10), pp. 1346-1357.

[15] Jamaati, J., Niazmand, H., and Renksizbulut, M., 2010, “Pressure-driven electrokinetic slip-flow in planar microchannels,” International Journal of Thermal Sciences, in press.

[16] Maynes, D., and Webb, B.W., 2003, “Fully developed electro-osmotic heat transfer in microchannels,” International Journal of Heat and Mass Transfer, 46, pp. 1359–1369.

[17] Jain, A., and Jensen, M. K., 2007, “Analytical modeling of electrokinetic effects on flow and heat transfer in microchannels,” International Journal of Heat and Mass Transfer, 50, pp. 1087–1096.

